THE JOURNAL OF BIOLOGICAL CHEMISTRY VOL. 287, NO. 33, pp. 27526–27536, August 10, 2012

Urokinase-type Plasminogen Activator-like Proteases in Teleosts Lack Genuine Receptor-binding Epidermal Growth Factor-like Domains*[S]

Received for publication, April 4, 2012, and in revised form, June 12, 2012 Published, JBC Papers in Press, June 25, 2012, DOI 10.1074/jbc.M112.369207

René Bager[‡§], Thomas K. Kristensen[‡], Jan K. Jensen[‡§], Agnieszka Szczur[‡§], Anni Christensen[‡§], Lisbeth M. Andersen[‡§], Jesper S. Johansen[‡], Niels Larsen[‡], Erik Baatrup[¶], Mingdong Huang[§‖], Michael Ploug[§], and Peter A. Andreasen[‡§1]**

*From the [‡]Department of Molecular Biology and Genetics and the [§]Danish–Chinese Centre for Proteases and Cancer, Aarhus University, 10 Gustav Wieds Vej, 8000 Aarhus C, Denmark, the [¶]Department of Bioscience, Zoophysiology, Aarhus University, Building 1131, 3 C.F. Moellers Allé, 8000 Aarhus C, Denmark, the [‖]Fujian Institute of Research on the Structure of Matter, Chinese Academy of Sciences, Fuzhou, China, and the **Finsen Laboratory, Rigshospitalet and Biotech Research and Innovation Center, Copenhagen Biocenter, 5 Ole Maaloes Vej, 2200 Copenhagen N, Denmark*

Background: In mammals, extracellular proteolysis initiated by urokinase-type plasminogen activator (uPA) is associated with cell surfaces via the uPA-receptor uPAR.
Results: Fish have two uPAs, one lacking the uPAR-binding domain, another having a uPAR-binding domain lacking two cysteines and a genuine uPAR-binding sequence.
Conclusion: In fish, uPA-dependent proteolysis occurs without uPAR.
Significance: Evolutionary studies provide a more comprehensive understanding of extracellular proteolysis.

Plasminogen activation catalyzed by urokinase-type plasminogen activator (uPA) plays an important role in normal and pathological tissue remodeling processes. Since its discovery in the mid-1980s, the cell membrane-anchored urokinase-type plasminogen activator receptor (uPAR) has been believed to be central to the functions of uPA, as uPA-catalyzed plasminogen activation activity appeared to be confined to cell surfaces through the binding of uPA to uPAR. However, a functional uPAR has so far only been identified in mammals. We have now cloned, recombinantly produced, and characterized two zebrafish proteases, zfuPA-a and zfuPA-b, which by several criteria are the fish orthologs of mammalian uPA. Thus, both proteases catalyze the activation of fish plasminogen efficiently and both proteases are inhibited rapidly by plasminogen activator inhibitor-1 (PAI-1). But zfuPA-a differs from mammalian uPA by lacking the exon encoding the uPAR-binding epidermal growth factor-like domain; zfuPA-b differs from mammalian uPA by lacking two cysteines of the epidermal growth factor-like domain and a uPAR-binding sequence comparable with that found in mammalian uPA. Accordingly, no zfuPA-b binding activity could be found in fish white blood cells or fish cell lines. We therefore propose that the current consensus of uPA-catalyzed plasminogen activation taking place on cell surfaces, derived from observations with mammals, is too narrow. Fish uPAs appear incapable of receptor binding in the manner known from mammals and uPA-catalyzed plasminogen activation in fish may occur mainly in solution. Studies with nonmammalian vertebrate species are needed to obtain a comprehensive understanding of the mechanism of plasminogen activation.

Plasminogen activators are serine proteases that catalyze the conversion of the extracellular zymogen plasminogen to the active serine protease plasmin. Plasmin in turn catalyzes degradation of extracellular matrix proteins like fibrin and laminin. In mammals, there are two types of plasminogen activators, urokinase-type plasminogen activator (uPA)[2] and tissue-type plasminogen activator (tPA). Plasminogen activation is strictly controlled temporally and spatially. Thus, secretion of tPA from endothelial cells can initiate intravascular fibrinolysis, securing blood vessel patency (for a review, see Ref. 1). Cell-specific uPA production can initiate localized extracellular matrix turnover (for a review, see Ref. 2). uPA-catalyzed plasminogen activation is believed to take place mainly on cell surfaces, where uPA accumulates due to high-affinity binding by the receptor, uPAR. uPAR also functions as an adhesion receptor due to its affinity to the extracellular matrix protein vitronectin. It may also regulate the activity of integrins. uPAR is a three-domain protein bound to cell surfaces by a glycosylphosphatidylinositol anchor (for a review, see Ref. 3). Plasminogen activator inhibitor-1 (PAI-1) is a fast and specific inhibitor of

* This work was supported by Danish Medical Research Council Grant 2107–040003, Danish National Research Foundation Grant 26-331-6, and Novo-Nordisk Foundation Grant R114-A11382 (to P. A. A.).
[S] This article contains supplemental Figs. S1–S6.
The nucleotide sequence(s) reported in this paper has been submitted to the GenBank™/EBI Data Bank with accession number(s) FJ660930 and HQ403602.
[1] To whom correspondence should be addressed: Dept. of Molecular Biology and Genetics, Aarhus University, 10 Gustav Wieds Vej, 8000 Aarhus C, Denmark. Tel.: 45-87155456; E-mail: pa@mb.au.dk.

[2] The abbreviations used are: uPA, urokinase-type plasminogen activator; *ef1α*, elongation factor 1-α; PAI-1, plasminogen activator inhibitor-1; S-2288, H-D-Ile-Pro-Arg-*p*-nitroanilide; S-2251, H-D-Val-Leu-Lys-*p*-nitroanilide; S-2444, pyroGlu-Gly-Arg-*p*-nitroanilide; tPA, tissue-type plasminogen activator; uPAR, urokinase-type plasminogen activator receptor; zfuPA-a, zebrafish urokinase-type plasminogen activator-like protease-a; zfuPA-b, zebrafish urokinase-type plasminogen activator-like protease-b; qPCR, quantitative PCR.

both plasminogen activators (for a review, see Ref. 4). uPAR-bound uPA·PAI-1 complex can be internalized and degraded by receptors of the low density lipoprotein receptor family (for reviews, see Refs. 4 and 5).

As listed from the N terminus, uPA from mammals has an epidermal growth factor (EGF)-like domain (residues 7–47 in human uPA), a kringle domain (residues 50–131 in human uPA), an interdomain linker (residues 132–147 in human uPA), and a C-terminal catalytic domain (in human uPA, residues 148–411 or 1–251 in the chymotrypsin template numbering). It is secreted as a single-chain proform or zymogen with an activity at least 250-fold lower than that of the fully active two-chain form, which is produced by cleavage of the $Lys^{158/15}$–$Ile^{159/16}$ bond (throughout the text, when double numbers separated by a slash are used to describe an amino acid position, the first number refers to the actual amino acid number while the second number refers to number of the corresponding amino acid in chymotrypsionogen.) After cleavage, residues 1–158/15 remain bound to the catalytic domain by a $Cys^{148/1}$–$Cys^{279/122}$ disulfide bond. No function has yet been assigned to the kringle domain (for a review, see Ref. 2). It is the EGF-like domain that binds to uPAR (6).

Plasminogen exists in all vertebrates (7, 8), but so far, plasminogen activation has been studied almost exclusively in mammals and birds, whereas reports describing direct characterization of plasminogen activators from lower vertebrates have been sparse. Takahashi *et al.* (9) reported that two antigens from platyfish (*Xiphophorus maculatus*) with M_r values of 50,000 and 55,000, respectively, cross-reacted with two monoclonal antibodies against human uPA; two major plasminogen activators, as detected by SDS-PAGE and fibrin-agarose zymography, migrated with similar M_r values. In goldfish, SDS-PAGE and casein zymography of homogenates of injured optic nerve revealed plasminogen activation activity migrating as two bands with M_r between 60,000 and 65,000 (10).

The sequencing of the genomes of vertebrate species beyond mammals and birds now allows more detailed biochemical studies into plasminogen activation in reptiles, amphibians, and bony fishes. Recently, both uPA-like and uPAR-like, but as yet unverified, sequences were found in the genome of the lizard *Anolis carolinensis*. There is no knowledge about uPA or uPAR in amphibians. For zebrafish (*Danio rerio*), the databases contain evidence for one plasminogen gene, one zebrafish tPA (zftPA) gene, and one zebrafish PAI-1 (zfPAI-1) gene, neither of which have any obviously striking differences from their mammalian counterparts. In contrast, we have found no evidence for a uPAR-like protein in teleosts in the sequence databases, and found two genes encoding proteins resembling mammalian uPA, which we will refer to as zebrafish urokinase-type plasminogen activator-like protease-a (zfuPA-a) and zebrafish urokinase-type plasminogen activator-like protease-b (zfuPA-b). Here, we present experimentally verified full-length cDNA sequences of zfuPA-a and zfuPA-b. These proteins have the unusual feature of either lacking of a growth factor domain or having a growth factor domain with an unusual sequence and an unusual disulfide bond connectivity. Accordingly, we were unable to identify binding activity on autologous cells for zebrafish uPAs. We therefore hypothesize that uPA-catalyzed plasminogen activation in fishes functions without an uPAR like that known from mammals.

EXPERIMENTAL PROCEDURES

RNA Extraction and Reverse Transcription—Sexually mature male and female zebrafish (*D. rerio*) were sacrificed by chilling on ice and dissected. Testis, ovary, liver, heart, gill, eye, and brain tissues were subsequently stored in RNAlater (Ambion, Austin, TX) to protect the RNA from degradation. Total RNA was isolated from the RNAlater preserved samples using the Qiagen RNeasy Mini Kit (Qiagen). This protocol included a DNase treatment step according to the manufacturer's recommendations to eliminate genomic DNA contamination. For cloning purposes, cDNA was generated from an mRNA pool extracted from testes of 16 adult zebrafish.

Derivatization of the zfuPA-a cDNA—Full-length zfuPAa cDNA was isolated and assembled from a total of 15 overlapping partial cDNA fragments. Six fragments were PCR amplified using primers designed from a published predicted partial zfuPA-a cDNA sequence (GenBank accession number XM_693024.2) that was identified by searching the NCBI protein database using human uPA. Although this sequence in its entirety was incorrectly predicted as demonstrated in the present study, part of the 3′-end of the sequence was correct and therefore useful for primer design. Six fragments were PCR amplified using primers that were designed from the published genomic sequence containing the putative zfuPA-a gene (GenBank accession number CR762430). A fragment including the entire coding region was finally PCR amplified to experimentally verify the sequence assembled from the fragments described above. The 5′- and 3′-ends were isolated using the SMART RACE cDNA Amplification Kit from Clontech together with the Advantage2 PCR Enzyme System (Clontech). For 5′- and 3′-RACE, nested PCR was used to amplify discrete RACE PCR products.

PCR fragments were isolated from agarose gels using the E.Z.N.A. Gel Extraction Kit (Omega Bio-tek) or the QIAquick Gel Extraction Kit (Qiagen) and cloned into the pCR2.1-TOPO or pCR4-TOPO vector using the TOPO TA Cloning system with the electrocompetent TOP10 *Escherichia coli* strain (Invitrogen). Sequencing reactions were performed using the BigDye Terminator version 3.1 Cycle Sequencing Kit (Applied Biosystems, Warrington, UK) with standard M13 forward and reverse primers and sequencing was performed on an ABI 3130 (Applied Biosystems) or an ABI 3730 XL (Applied Biosystems) by AGOWA (AGOWA, Berlin, Germany). The full cDNA sequence was deposited at GenBank (GenBank accession number FJ660930).

Derivatization of the zfuPA-b cDNA—Primers were designed to amplify most of the predicted coding sequence (GenBank accession number XM_001346681.2). The sequence was cloned and verified by sequencing and the full cDNA sequence was established using 3′- and 5′-RACE PCR as described above. In all cases, several individual clones were sequenced. The full cDNA sequence was deposited at GenBank (GenBank accession number HQ403602).

Sequence Analysis—Intron-exon structures of the zfuPA-a and zfuPA-b genes were determined from the genomic

sequences containing the genes (GenBank accession numbers NC_007124 and NC_007123, respectively) using Spidey (11). Unless otherwise stated, sequences were aligned using MUSCLE (12) with default parameters.

Quantitative Real-time PCR—Tissue levels of the zfuPA-a and zfuPA-b mRNAs were measured by real-time quantitative PCR. Real-time qPCR primers for use in SYBR Green assays were designed following the general recommendations on qPCR primer design with respect to base composition, secondary structures, amplicon lengths, and melting temperatures.

Quantification of zfuPA-a mRNA was performed using the primers CAGCACACTGGTTTGCCTAGA and TGCAGGCTGAAACATTACCCT (forward and reverse, respectively) spanning bases 1288–1393. Quantification of zfuPA-b mRNA was performed using the primers GGCAACATGATCACCGAGAA and GCATAAACACCAGGCCGAAA (forward and reverse, respectively) spanning base pairs 1295–1470.

PCR amplifications were performed in 96-well optical plates using the iQ SYBR Green Supermix (Bio-Rad) and relative gene expression was quantified with the MyiQ Real-time PCR Detection System (Bio-Rad) using the standard curve method. Real-time qPCR thermocycling conditions for zfuPA-a consisted of an initial denaturation at 95 °C for 3 min and 40 cycles of 95 °C for 10 s and 60 °C annealing/DNA synthesis for 45 s. For zfuPA-b, the conditions were 95 °C for 3 min and 40 cycles of 95 °C for 15 s and 62 °C for 45 s. The amplification was followed by a determination of amplicon melting temperature by denaturing at 95 °C for 1 min, reannealing at 55 °C for 1 min, and increasing the temperature 0.5 °C for every 10 s from 55 to 95 °C. All primer pairs amplified a single PCR product of the expected length when visualized on an agarose gel and produced a single well defined peak on amplicon melting curves and were therefore considered specific. To normalize the samples for variability in reverse transcription efficiency and RNA quality and quantity, relative zfuPA-a and zfuPA-b mRNAs levels were divided by relative elongation factor 1-α (*ef1*α; primer sequences in Ref. (13)) mRNA levels that showed very little variation across tissues.

Recombinant Production of zfuPA-a and zfuPA-b Protein—The full coding sequences of zfuPA-a and zfuPAb were cloned with C-terminal His_6 tags to the pTT5 vector, a derivative of the pTT vector (14). Suspension growing HEK293–6E cells (vector and cells kindly provided by Yves Durocher, NCR Biotechnology Research Institute, Montreal, Canada) were cultured in F17 medium (Invitrogen) supplemented with 0.1% Pluronic F-68 (Invitrogen), 4 mM L-Gln (Lonza), and 25 μg/ml of G418 (Invitrogen). Cells were transfected using $M_r \sim 25{,}000$ linear polyethylenimine (Polysciences), essentially as described elsewhere (15). Twenty-four hours post-transfection, Tryptone N1 (Organotechnie SAS) was added to a final concentration of 0.5% (w/v). Conditioned medium was collected 96 h post-transfection and the recombinant proteins were purified using immobilized metal ion affinity chromatography followed by size-exclusion chromatography. The purified proteins were at least 95% pure, as judged by Coomassie-stained SDS-PAGE (supplemental Fig. S1). The active, two-chain enzymes were produced by incubation with human or salmon plasmin followed by immobilized metal ion affinity chromatography. The activated proteins were at least 80% active as judged by Coomassie-stained SDS-PAGE after reaction with zebrafish PAI-1 (data not shown). Protein concentrations were determined from absorbance measurements using extinction coefficients calculated by the EXPASY ProtParam tool (16).

We introduced a K15A (chymotrypsinogen template numbering) mutation in zfuPA-a to ensure that it could be purified in the noncleaved form. As judged by silver staining after SDS-PAGE under reducing conditions, the purified material contained no detectable two-chain zfuPA-a (data not shown). zfuPA-b was purified exclusively in the noncleaved form, as judged by SDS-PAGE (data not shown) without the need for any mutations. ^{125}I-Labeled human uPA or zfuPA-b were prepared as described (17).

Recombinant PAI-1—Primers were designed to amplify the full coding sequence of zfPAI-1, using an available database sequence (GenBank accession number NM_001114559.1). The sequence was cloned and several individual clones were sequenced. The sequence was identical to the database sequence except for the stop codon that was located 24 bp later, corresponding to a C-terminal extension of the protein by 8 amino acid residues. The full coding sequence was cloned into the pTT5 vector and expressed in HEK293-6E as described above, and purified using ion-exchange chromatography followed by size exclusion chromatography. The purified protein was at least 95% pure as judged by Coomassie-stained SDS-PAGE (data not shown). Human PAI-1 (with the N-terminal His tag and heart muscle kinase recognition site) was expressed in *E. coli* as described (18). Active PAI-1 was purified from nonactive PAI-1 by affinity chromatography on immobilized β-anhydrotrypsin (19).

Fish Plasminogen—Fish plasminogen was purified from salmon plasma (Meridian Life Science, Inc., Saco, ME) by affinity chromatography on lysine-Sepharose 4B (GE Healthcare) according to Deutsch and Mertz (20). In Coomassie Blue-stained gels from nonreducing SDS-PAGE, the purified protein migrated as a M_r of ~85,000 band (data not shown). Human plasminogen was purified from human plasma by the same method.

Chromogenic Assays for uPA—The amidolytic activities of human uPA, zfuPA-a, and zfuPA-b were assayed using the chromogenic substrates S-2288 (Ile-Pro-Arg-*p*-nitroanilide) or S-2444 (pyro-Glu-Gly-Arg-*p*-nitroanilide) (Chromogenix). Assays were performed in 200-μl reaction volumes in a buffer consisting of 10 mM Hepes, 140 mM NaCl, pH 7.4, 0.1% BSA, incubated at 37 °C. The substrate turnover was followed by monitoring the optical density (OD) at 405 nm. For K_m measurements a dilution series of substrate ranging from 6 mM to 6 μM was incubated with 4 nM zfuPA-a, 2 nM zfuPA-b, or 4 nM human uPA. Initial reaction velocities (v_0) were calculated from the progress curves by linear regression. K_m and V_{max} were determined by fitting to the equation: $v_0 = (V_{max} \times [S])/(K_m + [S])$, where [S] represents the substrate concentration. k_{cat} values were calculated by dividing V_{max} with the enzyme concentration and using a conversion factor of 2.8854 OD/mM (determined from a standard curve of fully converted substrate).

K_i values were determined on the basis of assumption of simple Michaelis-Menten kinetics and competitive inhibition, using the equation: $V = (V_{max} \times [S])/([S] + K_m \times (1 + [I]_0/K_i))$,

where $[I]_0$ is the initial inhibitor concentration. The K_i values were estimated in either of two ways. The first way consisted in measuring apparent K_m values ($K_{m,obs}$) in the presence of different inhibitor concentrations and fitting to the equation $K_{m,obs} = K_m \times (1 + [I]_0/K_i)$. The second way consisted in measuring the apparent K_i values ($K_{i,obs}$) in the presence of different substrate concentrations and fitting to the equation: $K_{i,obs} = K_m \times (1 + [I]_0/K_i)$.

Second-order rate constants for inhibition by PAI-1 were determined essentially as described elsewhere (21) using substrates S-2444 and S-2288. Concentrations used were 2 nM human uPA, 25 nM human PAI-1, and 3 mM S-2444; 2 nM zfuPA-a, 75 nM human PAI-1, 3 mM S-2288; 1 nM zfuPA-b, 12.5 nM human PAI-1 and 3 mM S-2288; 2 nM human uPA, 75 nM zfPAI-1, 3 mM S-2444; 2 nM zfuPA-a, 25 nM zfPAI-1, and 6 mM S-2888; or 1 nM zfuPA-b, 12.5 nM zfPAI-1, 6 mM S-2288.

Analysis of Plasminogen Activation by SDS-PAGE—1 μM human or salmon plasminogen was incubated with 100 nM zfuPA-a, zfuPA-b, or human uPA at 37 °C in the presence of 1 μM aprotinin. After 0, 5, 10, 15, 20, 30, 60, and 120 min, samples corresponding to 3 μg of plasminogen were withdrawn and left on ice until analyzed by reducing SDS-PAGE (4–16%). The conversion of plasminogen to plasmin was quantified by using scanning densitometry, where the intensity of a high molecular weight band represented plasminogen and the combined intensity of two lower molecular weight bands represented plasmin.

uPA Binding Assays with Adherent Cell Lines—The zebrafish fibroblast-like cell lines ZF4 (22) and PAC2 (23) (both derived from zebrafish embryos; both kindly provided by Saskia Rueb, Leiden University, The Netherlands) were cultured at 28 °C in L-15 medium supplemented with 15% fetal bovine serum. Standard cell culture techniques and materials were used. PAC2 cells were detached using trypsin-EDTA, whereas ZF4 cells were only treated with trypsin. Cells were grown to confluence in 24-well multiwell plates and washed with PBS and incubated with 5 pM ^{125}I-labeled zfuPA-b in ice-cold binding buffer (10 mM Hepes, 140 mM NaCl, 2 mM $CaCl_2$, 1 mM $MgCl_2$, 1% BSA, pH 7.4) with or without 200 nM unlabeled zfuPA-b. After a 16-h incubation at 4 °C, the medium was collected. The cells were washed and solubilized in 1 M NaOH. Radioactivity in the medium and radioactivity associated with the cells was quantified using a γ-counter.

uPA Binding Assays with White Blood Cells—Human white blood cells were purified from ~50 ml of fresh, EDTA-treated blood, collected from two healthy male donors. Blood was diluted at a 1:1 ratio with phosphate-buffered saline (PBS) and overlaid on Ficoll-Paque Plus (GE Healthcare). After centrifugation (45 min, 400 × *g*, 20 °C), white blood cells were collected and washed twice in PBS before resuspension in PBS containing 1% bovine serum albumin (BSA). Cells were counted using a hemocytometer.

White blood cells from trout were purified from ~45 ml of fresh heparin and citrate-treated blood collected from one ~4 kg rainbow trout. Collected blood was stored on ice immediately after extraction and until centrifugation. White blood cells were isolated using a method modified from those previously published (24, 25). Blood were diluted 10:1 with 20 mM sodium phosphate, pH 7.2, 190 mM NaCl and interlaid in a discontinued Percoll gradient (density top layer 1.060 g/ml, and bottom layer 1.075 g/ml). Following centrifugation (40 min, 400 × *g*, 4 °C), the layer containing white blood cells was identified in a light microscope, collected, and the cells were counted.

For binding experiments, 1×10^6 cells were incubated with 3 pM ^{125}I-labeled zfuPA-b or human uPA. For competition, the single-chain forms of zfuPA-b or human uPA were used at a 200 nM concentration. The cells and the ligand were incubated in PBS containing 1% BSA for 3 h at 4 °C. Cells were collected by centrifugation and radioactivity in the medium and radioactivity associated with the cells was quantified using a γ-counter.

Homology Modeling—Homology models of the serine protease domains of zfuPA-a and zfuPA-b were generated by Swiss-Model (26) and docked onto the structure of human PAI-1 (PDB entry 3PB1).

Bioinformatic Search for uPAR Homologues—To find new uPAR representatives in the public databases, the most conserved uPA/uPAR sequence signatures were isolated and the search motifs created shown in Fig. S6. The UniProt (27) (July 2011 version) and Refseq (28) (version 48) were downloaded and indexed. The datasets were searched using Patscan (29) and Patscan output was converted to match tables with taxonomy taken from the databases. Less sensitive BLAST searches were also done against the nonredundant protein data banks at NCBI.

RESULTS

Plasminogen and Plasminogen Activator-like Genes in the Zebrafish Genome—A search of the databases using BLAST revealed one zebrafish plasminogen gene, one zebrafish tPA gene, and one zebrafish PAI-1 gene, which displayed no immediately striking differences from their mammalian counterparts (data not shown). In contrast, there are two genes similar to mammalian uPA, both containing a genuine serine protease catalytic domain and an N-terminal extension. We decided to verify that the two genes encode the fish counterparts of uPA by cloning full-length cDNAs and expressing the proteins for both. We will refer to them as zfuPA-a and zfuPA-b.

Sequence Analysis of zfuPA-a—The zfuPA-a mRNA is 2408 base pairs long and is comprised of 11 exons. The gene spans 7923 base pairs (introns and exons) on zebrafish chromosome 13. The coding sequence starts in exon 2 and stops within exon 11. The predicted translation start codon corresponds to a 402-amino acid long open reading frame before a stop codon is encountered. Upstream from the predicted translation start codon, an in-frame stop codon can be found, ruling out any other potential translation start codons upstream of the predicted one.

Most exons of the fish gene coincided with the corresponding exons in human uPA gene (*PLAU*), except for two notable features. First, the linker between the kringle and the catalytic domain was encoded by an extra exon in zfuPA-a; second, the exon corresponding to the exon encoding the EGF-like domain in human uPA is lacking in zfuPA-a (Fig. 1). Knowing that the cDNA sequence is full-length rules out the possibility of an EGF-like domain-encoding exon further upstream.

Another unusual feature of zfuPA-a is the occurrence of cysteines in the kringle. Compared with the human uPA kringle,

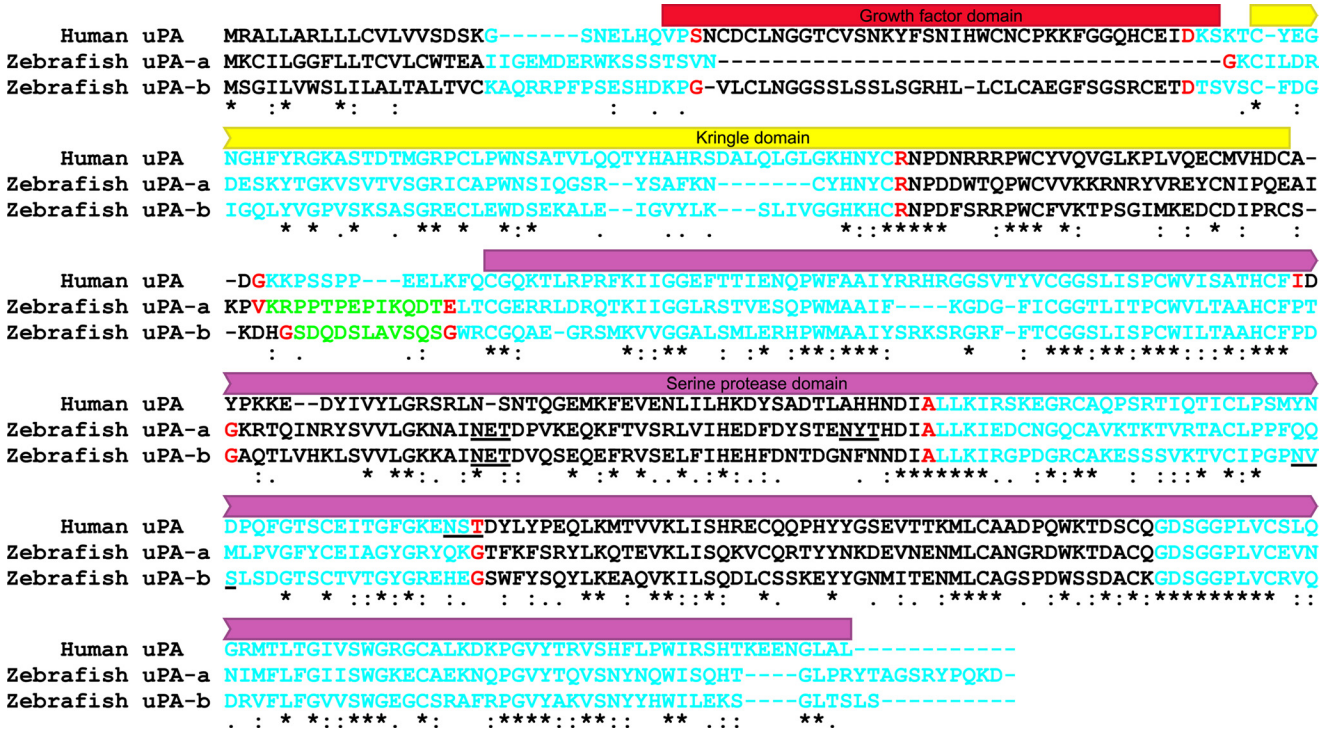

FIGURE 1. **Exon-intron structure of the genes for human uPA, zfuPA-a, and zfuPA-b.** The exons of human uPA are colored alternating *black* and *blue*. The corresponding exons of the zfuPA-a and zfuPA-b are colored likewise. Extra exons in the zfuPA-a and zfuPA-b are colored *green*. *Red* indicates residues encoded across splice sites. The degree of sequence conservation is indicated by *asterisks* (fully conserved), colons (strongly conserved), and full stops (weak). *Colored bars* indicate the domains of human uPA. Potential *N*-linked glycosylation sites are *underlined*.

the zfuPA-a kringle is lacking the most C-terminal cysteine. Instead, zfuPA-a has an additional cysteine in a position between cysteines 2 and 3 from the N terminus of the human uPA kringle. In human uPA, all kringle cysteines are part of disulfide bridges and the kringle of zfuPA-a therefore must have a different disulfide bridge pattern (Fig. 1). However, this unusual occurrence of cysteines was not seen in other fish species (supplemental Fig. S2) and was not studied further. zfuPA-a has two potential glycosylation sites, at Asn^{76}/227 and $Asn^{97/248}$, which are both different from the single glycosylation site in human uPA, at $Asn^{145/302}$.

Sequence Analysis of zfuPA-b—The zfuPA-b mRNA is 2299 bp long. The gene, which is located on chromosome 12, is comprised of 14 exons. The gene spans 18,577 base pairs (introns and exons) on zebrafish chromosome 12. The coding sequence starts in exon 4 and stops within exon 15. The predicted translation start codon corresponds to a 432-amino acid long open reading frame before a stop codon is encountered. Like for zfuPA-b, the start codon is verified by the presence of an in-frame stop codon upstream from the start codon.

Compared with human uPA, zfuPA-b contained an extra exon in the linker between the kringle domain and the catalytic domain. The exon encoding the growth factor domain of zfuPA-b differs from that of mammalian uPA by the fact that two cysteines are missing in zfuPA-b. Moreover, the sequence of the growth factor domain of zfuPA-b (LSSSLSGHRLL) corresponding to the uPAR binding sequence of human uPA (VSNKYFSNIHW; residues important for binding to uPAR underlined) consisted almost exclusively of short aliphatic residues, in contrast to the human sequence, which is rich in aromatic and charged residues at the positions important for binding to uPAR (Fig. 1). zfuPA-b contained a potential glycosylation site at $Asn^{76/227}$, identical to one of the potential glycosylation sites in zfuPA-a.

Sequence Comparison to tPA—We aligned the sequences of the catalytic domains of zfuPA-a and zfuPA-b and zftPA with their human counterparts and compared characteristic features. First, human uPA has a Lys before the activation cleavage site, whereas human tPA has an Arg. In this respect, zfuPA-a and zfuPA-b as well as zftPA are identical to their human counterparts (Fig. 2). Second, a characteristic of mammalian tPA is a basic residue in the 2nd position after the activation cleavage site. This feature is also shared by zftPA, but not by zfuPA-a or zfuPA-b (Fig. 2). Third, the tPAs have long 37-loops (the loop at the amino acid position that corresponds to amino acid 37 in chymotrypsinogen), whereas the uPAs have shorter ones (Fig. 2). Fourth, the N-terminal extension of all the tPAs contain, as mentioned from the N terminus, a fibronectin finger domain, a growth factor domain, and two kringles (data not shown). This domain organization is clearly different from that of any of the uPAs (see above). We can therefore conclude that zfuPA-a and zfuPA-b show more sequence resemblance to human uPA than to zftPA, whereas zftPA show more sequence resemblance to human tPA than to zfuPA-a and zfuPA-b.

Tissue-specific Expression of zfuPA-a and zfuPA-b mRNA—Tissue-specific expression of the uPA genes was characterized in adult zebrafish, using real-time qPCR with primers spanning bases 1288–1393 and 1295–1470 (zfuPA-a and zfuPA-b, respectively, and counted from the translation start codon) (Fig. 3). The expression in the gonads displayed a strong sexual dimorphism, zfuPA-a

```
                          Activation
                         cleavage site
                               ↓                          37-loop
     Human tPA   QCGLRQ---YSQPQFRIKGGLFADIASHPWQAAIFAKHRRSPGERFLC
Zebrafish tPA    TCGQRESPSNLLPMFRIRGGQASDIREQPWQAAITVYLPRSKTHNFLC
     Human uPA   VCGQKT----LRPRFKIIGGEFTTIENQPWFAAIYRRH-RGGSVTYVC
Zebrafish uPA-a  TCGERR----LDRQTKIIGGLRSTVESQPWMAAIFK------GDGFIC
Zebrafish uPA-b  RCGQAE-----GRSMKVVGGALSMLERHPWMAAIYSRK--SRGRFFTC
```

FIGURE 2. **Comparison of zebrafish and human uPAs and tPAs.** The N-terminal part of the catalytic domains from uPAs and tPAs are aligned. The activation cleavage site and the 37-loop are labeled. Differences between the activation cleavage sites of tPAs and uPAs are highlighted with different *shades of gray*.

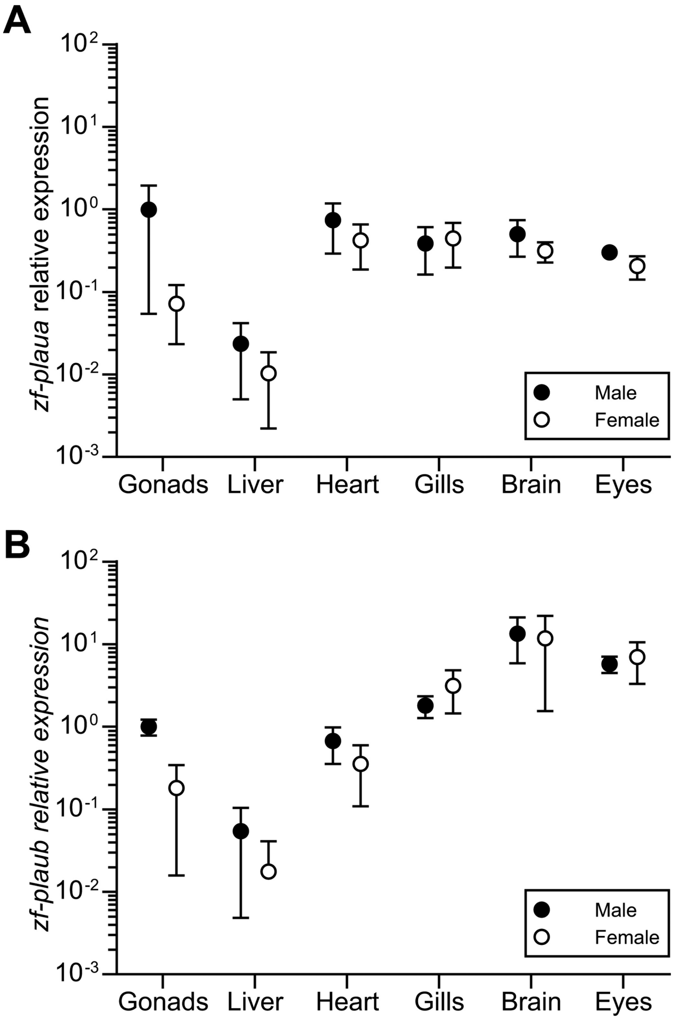

FIGURE 3. **Levels of zfuPA-a and zfuPA-b mRNAs in zebrafish tissue.** Relative mRNA levels were determined by qPCR and normalized to the *ef1α* mRNA levels. Each data point represents mean ± S.D. values for tissues from six individuals. For each gene, data were normalized to the level in testes. Values on the *y* axes are arbitrary units corresponding to a standard curve of diluted mRNA and the two graphs are thus not directly comparable. *A*, expression levels of *zfplau-a* (the gene encoding zfuPA-a). *B*, expression levels of *zfplau-b* (the gene encoding zfuPA-b).

and zfuPA-b mRNA levels in testis being about 10-fold higher than those in the ovary. Such a sexual dimorphism was not observed for any of the other tissues. The zfuPA-a and zfuPA-b mRNA expression levels in heart, gill, brain, and eye were all similar, whereas male and female liver zfuPA-a and zfuPA-b mRNA levels were ~20-fold lower than those in the four other tissues.

Enzymatic Properties of Recombinant zfuPA-a and zfuPA-b—For a quantitative estimation of the plasminogen activation activity of zfuPA-a and zfuPA-b, we incubated 1 μM plasminogen with 100 nM uPA at 37 °C. After incubation for various periods of time, the fraction of plasminogen converted to plasmin was estimated by SDS-PAGE under reducing conditions and densitometric scanning of the Coomassie Blue-stained gels. We combined zfuPA-a and zfuPA-b with salmon and human plasminogen, and human uPA with salmon and human plasminogen. zfuPA-a and zfuPA-b converted fish plasminogen to plasmin as efficiently as human uPA converted human plasminogen to plasmin. In contrast, there was little if any activity of zfuPA-a and zfuPA-b toward human plasminogen and human uPA against salmon plasminogen (Fig. 4). We therefore conclude that zfuPA-a and zfuPA-b are efficient plasminogen activators.

We determined the K_m and k_{cat} values for zfuPA-a and zfuPA-b catalyzed hydrolysis of the chromogenic substrates S-2288 and S-2444 (Table 1). With S-2444, zfuPA-b displayed somewhat higher K_m values than zfuPA-a and human uPA, but then again, also displayed higher k_{cat} values, so that the k_{cat}/K_m values were almost identical in all cases. With S-2288, the k_{cat}/K_m value for human uPA was about 10-fold lower than for the two fish uPAs.

Human uPA is secreted as a single-chain form with an activity that is at least 250-fold lower than that of the two-chain form (30). We therefore compared the activities of single-chain and two-chain forms of zfuPA-a and zfuPA-b (Fig. 5). In both cases, we were not able to detect any enzymatic activity of the single-chain forms. The sensitivity of the assays allows us to conclude that the activities of the single-chain forms are at least 200-fold lower than that of the two-chain forms. In contrast, mammalian single-chain tPA has an easily measurable activity that is only 10–50 lower than that of the two-chain form (31).

Second-order Rate Constants for Reaction of zfuPA-a and zfuPA-b with PAI-1—Each of the two zfuPAs could form an SDS-resistant complex with zfPAI-1 or human PAI-1 (supplemental Fig. S3), like also found for other protease-serpin pairs. The second-order rate constants for reaction of human uPA, zfuPA-a, and zfuPA-b with human PAI-1 were almost identical, around 5×10^6 M^{-1} s^{-1}. zfPAI-1 reacted with a similar rate with human uPA, but interestingly, about 10-fold faster with zfuPA-a and zfuPA-b (Table 2).

Susceptibility of Recombinant zfuPA-a and zfuPA-b to Synthetic Inhibitors—zfuPA-a and zfuPA-b were found to be as susceptible to the nonspecific serine protease inhibitor *p*-aminobenzamidine as human uPA (Table 3). Amiloride is known as an inhibitor of mammalian uPA, whereas mammalian tPA is not sensitive (32). The K_i value for inhibition by amiloride was almost 100-fold higher for zfuPA-a than for human uPA, whereas zfuPA-b was almost as susceptible to amiloride as human uPA (Table 3). zfuPA-a or zfuPA-b were not susceptible to inhibition by polyclonal antibodies raised against and inhibiting the enzyme activity of human uPA (data not shown).

Binding to zfuPA-b to Intact Fish Cell Lines and Fish White Blood Cells—There was no measurable saturable binding of ^{125}I-labeled zfuPA-a to trout white blood cells (Fig. 6) or zebrafish cell lines (supplemental Fig. S4). The choice of

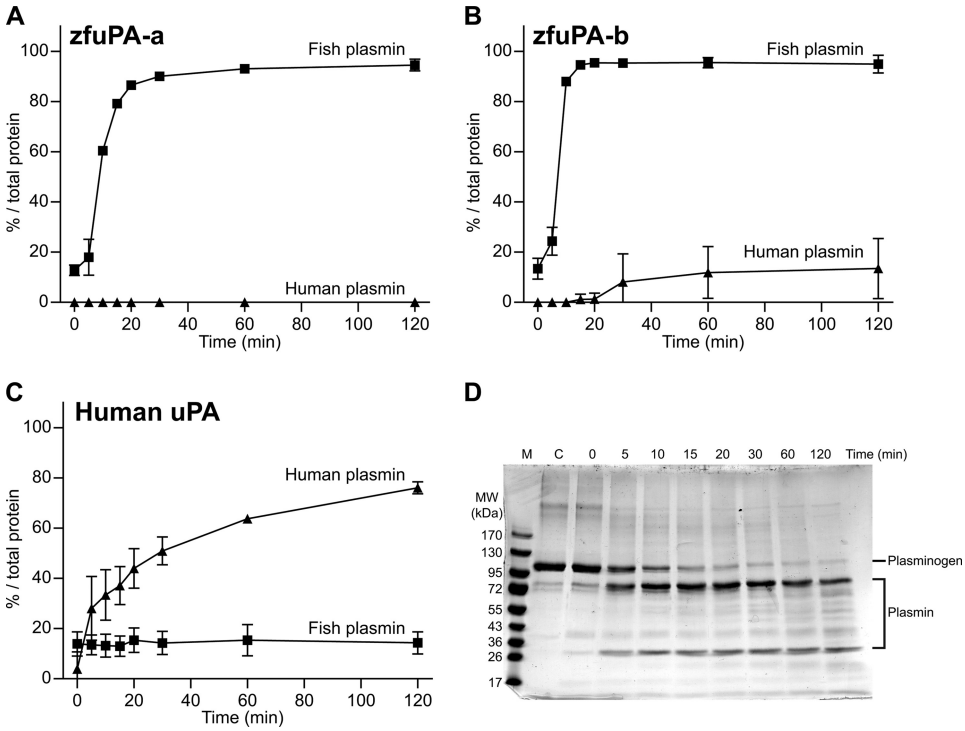

FIGURE 4. **Activation of human or salmon plasminogen by human uPA or zfuPA-a or zfuPA-b.** Salmon or human plasminogen (1 μM) was incubated with human uPA or zfuPA-a or zfuPA-b (100 nM) at 37 °C. At the indicated time points, 30-μl samples were taken for SDS-PAGE under reducing conditions. After electrophoresis, the gels were stained with Coomassie Blue and dried. The relative intensities of the plasminogen, plasmin heavy chain, and plasmin light chain were determined by densitometric scanning. The fraction of the added plasminogen, which had been converted plasmin, was calculated and plotted *versus* the incubation time (*closed squares*, fish plasmin; *closed triangles*, human plasmin). *Error bars* indicate S.D. calculated from three independent experiments. *A*, activation by zfuPA-a. *B*, activation by zfuPA-b. *C*, activation by human uPA. *D*, typical SDS-PAGE showing the activation of fish plasminogen by zfuPA-a (*MW*, molecular weight marker; *C*, control without addition of zfuPA-a).

TABLE 1

Catalytic activity of uPAs toward the chromogenic substrates S-2288 and S-2444

Values are reported as mean ± S.D. Numbers in parentheses indicate the number of independent determinations.

Substrate	Enzyme	K_m	k_{cat}	k_{cat}/K_m
		μM	s^{-1}	$s^{-1}{}_M{}^{-1}$
S-2288	zfuPA-a	44 ± 2 (3)	23 ± 1 (3)	(5.3 ± 0.04) × 10^5 (3)
	zfuPA-b	85 ± 15 (4)	52 ± 14 (4)	(6.1 ± 1.4) × 10^5 (4)
	Human uPA	406 ± 18 (5)	23 ± 8 (5)	(5.6 ± 1.9) × 10^4 (5)
S-2444	zfuPA-a	100 ± 3 (3)	28 ± 1 (3)	(2.8 ± 0.1) × 10^5 (3)
	zfuPA-b	512 ± 25 (4)	136 ± 27 (4)	(2.7 ± 0.6) × 10^5 (4)
	Human uPA	73 ± 0.4 (3)	25 ± 4 (3)	(3.4 ± 0.5) × 10^5 (3)

white blood cells for attempts to detect a fish uPAR was based on the fact that human white blood cells express abundant uPAR (33).

The absence of measurable binding limits the possibility for the existence of high affinity zfuPA-b binding receptors on the surface of fish white blood cells. Assuming a simple 1:1 binding equilibrium, a bound-to-free ratio sensitivity of 0.005, and with 1,000,000 cells per 1 ml, the upper limit to the number of receptors per cell can be calculated as follows: 300 receptors per cell, if K_D is 0.1 nM; 3000 receptors per cell, if K_D is 1 nM; 30,000 receptors per cell, if K_D is 10 nM; 300,000 receptors per cell, if K_D is 100 nM. These values should be compared with about 100,000 receptors per cell on human white blood cells with a K_D of 0.27 nM (33). Similar considerations hold true for the experiments with zebrafish cell lines (supplemental Fig. S4). Thus, we can conclude that if zfuPA-b does bind to a cellular receptor on the tested cell types, the affinity or the receptor number per cell have to be considerably lower than for receptor binding of uPA in mammals.

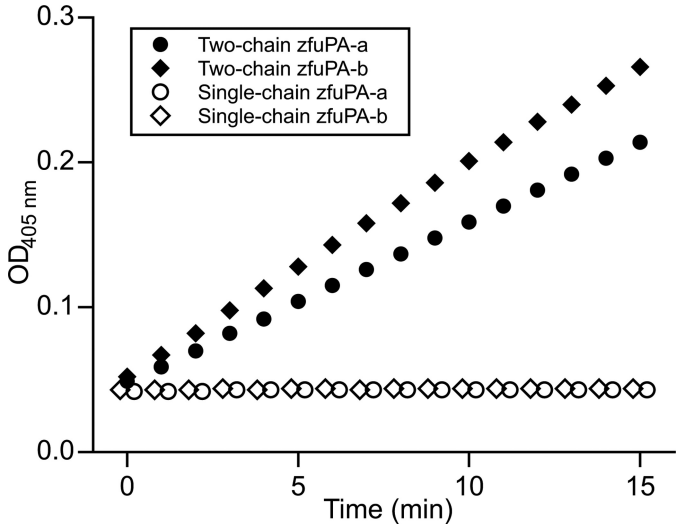

FIGURE 5. **Assay of the relative activities of the single-chain forms and the two-chain forms of zfuPA-a and zfuPA-b.** Four nM enzyme was incubated with 100 μM of the chromogenic substrate S-2288. The activities of two-chain zfuPA-a (*closed circles*), two-chain zfuPA-b (*closed diamonds*), single-chain zfuPA-a (*open circles*), and single-chain zfuPA-b (*open diamonds*) are shown. $A_{405\ nm}$, optical density at 405 nm.

DISCUSSION

In this report, we describe cloning, recombinant production, and characterization of two serine proteases, zfuPA-a and

TABLE 2

Second-order rate constants for inhibition of human uPA, zfuPA-a, and zfuPA-b by human PAI-1 and zfPAI-1

Values are reported as mean ± S.D. Numbers in parentheses indicate the number of independent determinations.

Enzyme	Human PAI-1	zfPAI-1
	k_2 ($\mu M^{-1} s^{-1}$)	k_2 ($\mu M^{-1} s^{-1}$)
Human uPA	4.4 ± 0.3 (3)	1.7 ± 0.1 (3)
zfuPA-a	2.5 ± 0.03 (3)	17 ± 1.0 (3)
zfuPA-b	7.5 ± 0.5 (3)	15 ± 1.4 (3)

TABLE 3

Susceptibility of zfuPA-a and zfuPA-b to general serine protease inhibitors

K_i values for inhibition by *p*-amino-benzamidine and amiloride are reported as mean ± S.D. Numbers in parentheses indicate the number of independent determinations.

Enzyme	K_i, *p*-amino-benzamidine	K_i, amiloride
	μM	
Human uPA[a]	40 ± 11 (3)	5 ± 1 (3)
zfuPA-a	88 ± 10 (3)	421 ± 196 (3)
zfuPA-b	42 ± 2 (3)	24 ± 2 (3)
zftPA	Not determined	>2000

[a] The values for human uPA were those previously reported (49).

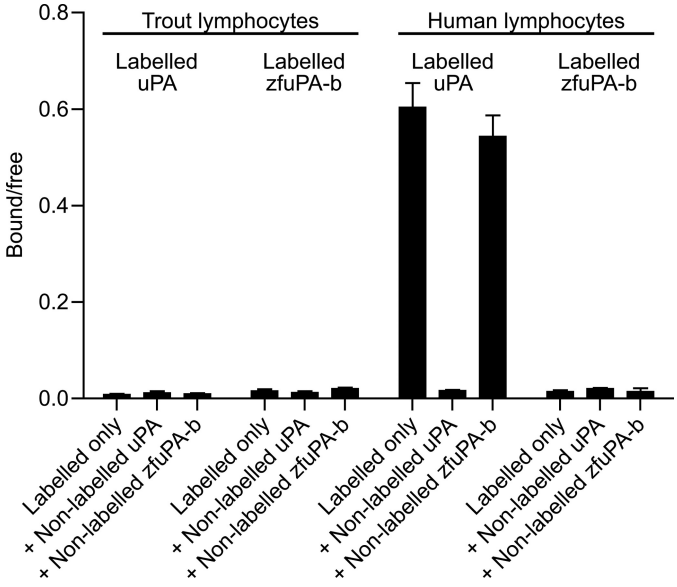

FIGURE 6. **Assay of binding of human or fish uPA to human or fish lymphocytes.** The binding of ^{125}I-labeled uPA or ^{125}I-labeled zfuPA-b to lymphocytes isolated from human blood or rainbow trout blood was estimated by incubating cells with 5 pM labeled uPA, in the presence or absence of 200 nM nonlabeled human uPA or nonlabeled zfuPA-b. The ratio between bound and free labeled ligand is reported. *Error bars* represents S.D. for 3 independent determinations.

zfuPA-b, from zebrafish. On the basis of a number of characteristics, we conclude that the two serine proteases represent the fish orthologs of mammalian uPA, but that they differ from that with respect to the EGF-like domain.

It is interesting to note, although, that zfuPA-a and zfuPA-b are poor activators of human plasminogen and human uPA a poor activator of salmon plasminogen. This difference may at least partially be related to a difference in the amino acid present in the P3 position in the activation loop of plasminogen, the activation loop of human plasminogen having a Pro and the activation loop of fish plasminogen a Phe in this position.

The existence of two uPA genes seems to be a general feature for teleosts, as suggested by alignment of several fish uPA sequences deposited in the databases (supplemental Fig. S2). uPA-like serine proteases in these fish species can be classified as belonging to either the a or b type, on the basis of the length of their 37-loop, *i.e.* the stretch between Phe or Tyr in position 34 and Phe or Tyr in position 40. As far as the catalytic domains are concerned, the two zfuPAs are closer to each other than either of them are to human uPA. They have one common potential glycosylation site, different from that of human uPA. In addition, both have an additional exon in the linker between the kringle and the catalytic domain.

Both active site and exosites of uPA are important for interaction with PAI-1, as revealed by the three-dimensional structure of the human uPA-human PAI-1 Michaelis complex (34). Among the exosites, the 37-loop plays a pivotal role. In human uPA, this loop is relatively long, compared with other serine proteases, allowing it to adopt an extended conformation and make strong contacts with the β-sheet C of PAI-1. The 37-loop in zfuPA-b is only 1 residue shorter than that in human uPA, but the 37-loop of zfuPA-a is 5 residues shorter. Nevertheless, zfuPA-a and zfuPA-b react with human PAI-1 with identical second-order rate constants. Docking homology models of the serine protease domains of zfuPA-a and zfuPA-b onto the structure of human PAI-1 showed an interaction surface between zfuPA-b and PAI-1 similar to that between human uPA and PAI-1 (data not shown), whereas zfuPA-a, having a short 37-loop, instead has a 2-residue longer 60-loop, with residue Lys^{60c} able to interact with PAI-1 residue Glu^{212} in β-sheet C (supplemental Fig. S5). These results are consistent with the similar reaction rates of zfuPA-a, zfuPA-b, and human uPA with human PAI-1.

The most important difference between the two fish uPAs and mammalian uPA concerns the EGF-like domain. Fish uPA-a lacks an EGF-like domain. The EGF-like domain of fish uPA-b lacks Cys^{11} and Cys^{19}, which are connected by a disulfide bond in EGF-like domains in general, also in the EGF-like domain of uPA of the tetrapods (Fig. 7 and supplemental Fig. S2). In tetrapod uPA, the Cys^{11}–Cys^{19} disulfide bond is adjacent to the Ω-loop between positions 23 and 29, which has been implicated in the direct contact of uPA to uPAR in mammals (35–38). The corresponding sequence in EGF itself is likewise decisive for binding to EGF receptors (35). To the best of our knowledge, there are no mutagenesis studies unambiguously probing the functional importance of the Cys^{11}-Cys^{19} disulfide bond in human uPA. Only, a fragment of the human uPA EGF-like domain, covering residues 12–32 and with a Cys19Ala mutation and thus lacking the Cys^{11}-Cys^{19} bond, had an about 200-fold reduced uPAR-binding affinity, in agreement with the expectances from a hypothesis of importance of this disulfide bond for uPAR binding. Aminobutyric acid substitution of the first and third Cys residue of murine EGF, corresponding to Cys^{11} and Cys^{19} of human uPA, rendering them unable to form a disulfide bond, led to a more than 100-fold reduction in biological activity and receptor-binding affinity (39). This disulfide bond thus seems important for maintaining a functional state of the receptor binding loop of EGF-like domains.

In the uPA EGF-like domain of mammals, birds, and reptiles, the uPAR-binding Ω-loop (residues 23–29) contains a number of charged and hydrophobic residues that participate in the

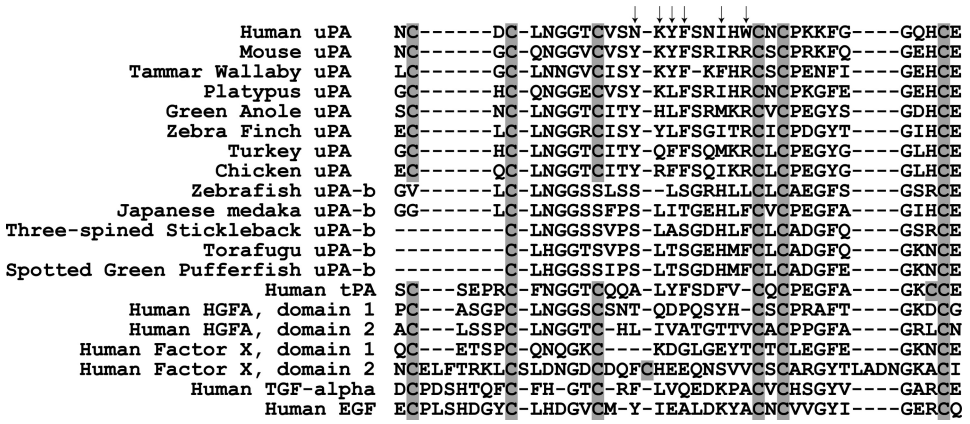

FIGURE 7. **Alignment of uPA EGF-like domains from selected amniotes and fishes and other EGF-like domains.** Cysteines are highlighted in *gray*. Residues important for the binding between human uPA and human uPAR are indicated by *arrows*.

binding to uPAR (Fig. 7) (36–38). In contrast, the corresponding fish sequence is rich in small aliphatic and hydrophilic residues (LSSLSGHRLL in zebrafish), unlikely to be able to support protein-protein interactions (Fig. 7). On this basis, we conclude that fish uPA-a is certainly and uPA-b most likely unable to bind to a receptor in the manner in which mammalian uPA binds to mammalian uPAR.

Moreover, we observed no measurable binding of zfuPA-b to intact cells, neither cultured zebrafish cells nor white blood cells from trout blood. On the basis of the sensitivity of the binding assay, we are confident that the tested cell types do not possess high affinity receptors for zfuPA-b, *i.e.* receptors binding zfuPA-b with a K_D in a low nanomolar or picomolar range. Obviously, the extrapolation of this conclusion to a general statement about nonexistence of a fish uPAR is restricted by the fact that only two zebrafish cell lines were available. Also, we had to do binding experiments with uPA from zebrafish and white blood cells from trout, because these cells, in contrast to zebrafish white blood cells, can be obtained in sufficient quantitites. We cannot rule out the possibility that the lack of detectable binding may be caused by the crossing of the species barrier with a resulting lower affinity and poorer sensitivity. Nevertheless, despite our attempts to do so, we have not been able to disprove our hypothesis of a lack of fish uPAR.

We performed a search for uPAR-like sequences in fish species on the basis of the disulfide bond pattern in mammalian uPAR and on the fact that all three domains of uPAR are functionally important for uPA binding (40). We searched the Uniprot and Refseq databases with algorithms designed to detect 2- or 3-domain proteins with the disulfide bond pattern that is conserved at the C terminus of each domain of human uPAR (supplemental Fig. S6). The search faithfully picked up uPAR from mammalian species. We also identified an *A. carolinensis* sequence likely to represent a reptile uPAR. But although the search did yield fish sequences fulfilling the search criteria, a closer inspection revealed that none of them were related to mammalian uPAR (data not shown). Thus, despite performing an elaborate search, we were unable to identify fish proteins fulfilling the conditions for being a uPA binding homologue of mammalian uPAR. The lack of cell biological and bioinformatic evidence for the existence of a fish homolog of mammalian uPAR is in good agreement with the lack or dissimilarity of the EGF-like domains in the fish uPAs.

Although serine peptidase enzyme systems have been extensively studied in mammals, there is much less information about other chordate species. Two rounds of whole genome duplications and neofunctionalization of the duplicate genes occurred in the vertebrate subphylum after divergence from the other chordate subphyla, the lancelets and tunicates, allowing the development of the more complex vertebrate organisms, for instance, with a true blood circulatory system and thrombin-catalyzed fibrin clotting (8, 41, 42). Also the origin of the plasminogen activation system shall most likely be sought among the primitive chordates. None of the components of the fibrinolytic system have been found in the known tunicate and lancelet genomes (7, 8). Because EGF-like domains in general contain 6 Cys and a conserved disulfide bond pattern (for a review, see Ref. 43), we propose an archaic uPA with an EGF-like domain with 6 Cys. The existence of the two uPA genes in fish is in good agreement with the fact that a whole genome gene duplication occurred in the teleost subsequent to its divergence from other vertebrates (44). The fact that both fish uPAs seem to lack the capability for uPAR binding, but by different mechanisms, is in agreement with the apparent lack of uPAR in fishes. We propose that an archaic uPA and an archaic uPAR initially arose independently in the vertebrate phylum, mutations in each gene creating a new interaction surface during the evolution of the vertebrates. Whether a functional uPA-uPAR binding existed in the last common ancestor of teleosts and tetrapods is a question that can be elucidated by searching for uPA- and uPAR-like molecules in chondrichthyes and agnatha. But because of our observations with teleosts, we consider it most likely that functional uPA-uPAR binding is a feature of the tetrapods. It is also interesting to notice that uPAR-independent functions of uPA have been reported in mammals, including in vascular wound healing (45) and induction of cardiac fibrosis (46), and also uPA-independent functions of uPAR, including modification of kidney barriers in sepsis (47) and activation of formyl peptide receptors (48). Thus, each gene product seems to maintain some of the original independent functions they may originally have had in lower vertebrates.

The results presented here suggest that the focus on the functions of plasminogen activation in mammals, due to its relevance to human pathophysiology and the availability of targeted gene deletions in mice, may have given a too narrow picture of the mechanism of action of the system. Studies in nonmammalian species are needed to obtain a comprehensive understanding of the biochemistry and cell biology of plasminogen activation. The two fish gene products described fulfill a minimum requirement for having a biological function, namely by being expressed in the fish. Obviously, establishment of their exact biological functions will have to await functional studies with specific gene deletions and exact determinations of cell types expressing them.

REFERENCES

1. Collen, D. (1999) The plasminogen (fibrinolytic) system. *Thromb. Haemost.* **82,** 259–270
2. Andreasen, P. A., Kjøller, L., Christensen, L., and Duffy, M. J. (1997) The urokinase-type plasminogen activator system in cancer metastasis. A review. *Int. J. Cancer* **72,** 1–22
3. Kjaergaard, M., Hansen, L.V., Jacobsen, B., Gardsvoll, H., and Ploug, M. (2008) Structure and ligand interactions of the urokinase receptor (uPAR). *Front. Biosci.* **13,** 5441–5461
4. Dupont, D. M., Madsen, J. B., Kristensen, T., Bodker, J.S., Blouse, G. E., Wind, T., and Andreasen, P. A. (2009) Biochemical properties of plasminogen activator inhibitor-1. *Front. Biosci.* **14,** 1337–1361
5. Gliemann, J., Nykjaer, A., Petersen, C. M., Jørgensen, K. E., Nielsen, M., Andreasen, P. A., Christensen, E. I., Lookene, A., Olivecrona, G., and Moestrup, S. K. (1994) The multiligand α_2-macroglobulin receptor/low density lipoprotein receptor-related protein (α2MR/LRP). *Ann. N.Y. Acad. Sci.* **737,** 20–38
6. Appella, E., Weber, I. T., and Blasi, F. (1988) Structure and function of epidermal growth factor-like regions in proteins. *FEBS Lett.* **231,** 1–4
7. Jiang, Y., and Doolittle, R. F. (2003) The evolution of vertebrate blood coagulation as viewed from a comparison of pufferfish and sea squirt genomes. *Proc. Natl. Acad. Sci. U.S.A.* **100,** 7527–7532
8. Doolittle, R. F. (2009) Step-by-step evolution of vertebrate blood coagulation. *Cold Spring Harbor Symp. Quant. Biol.* **74,** 35–40
9. Takahashi, K., Wakamatsu, Y., Ozato, K., and Wakayama, Y. (1987) Fish plasminogen activators, their identification and characterization. *Cell Struct. Funct.* **12,** 11–22
10. Sallés, F. J., Schechter, N., and Strickland, S. (1990) A plasminogen-activator is induced during goldfish optic nerve regeneration. *EMBO J.* **9,** 2471–2477
11. Wheelan, S. J., Church, D. M., and Ostell, J. M. (2001) Spidey. A tool for mRNA to genomic alignments. *Genome Res.* **11,** 1952–1957
12. Edgar, R. C. (2004) MUSCLE, multiple sequence alignment with high accuracy and high throughput. *Nucleic Acids Res.* **32,** 1792–1797
13. Alberti, M., Kausch, U., Haindl, S., Leibiger, R., Budczies, J., Seifert, M., and Hock, B. (2005) Gene expression patterns, a tool for bioanalysis. *Int. J. Environ. Anal. Chem.* **85,** 589–608
14. Durocher, Y., Perret, S., and Kamen, A. (2002) High-level and high-throughput recombinant protein production by transient transfection of suspension-growing human 293-EBNA1 cells. *Nucleic Acids Res.* **30,** E9
15. Tom, R., Bisson, L., and Durocher, Y. (2008) Transfection of HEK293-EBNA1 cells in suspension with linear PEI for production of recombinant proteins. *CSH Protoc.* 2008, 10.1101/pdb.prot4977
16. Gasteiger, E., Hoogland, C., Gattiker, A., Duvaud, S., Wilkins, M. R., Appel, R. D., and Bairoch, A. (2005) Protein identification and analysis tools on the ExPASy server. *The Proteomics Protocols Handbook*, pp. 571–607, Humana Press, Inc., NJ
17. Jensen, P. H., Christensen, E. I., Ebbesen, P., Gliemann, J., and Andreasen, P. A. (1990) Lysosomal degradation of receptor-bound urokinase-type plasminogen activator is enhanced by its inhibitors in human trophoblastic choriocarcinoma cells. *Cell Regul.* **1,** 1043–1056
18. Madsen, J. B., Dupont, D. M., Andersen, T. B., Nielsen, A. F., Sang, L., Brix, D. M., Jensen, J. K., Broos, T., Hendrickx, M. L., Christensen, A., Kjems, J., and Andreasen, P. A. (2010) RNA aptamers as conformational probes and regulatory agents for plasminogen activator inhibitor-1. *Biochemistry* **49,** 4103–4115
19. Blouse, G. E., Perron, M. J., Kvassman, J. O., Yunus, S., Thompson, J. H., Betts, R. L., Lutter, L. C., and Shore, J. D. (2003) Mutation of the highly conserved tryptophan in the serpin breach region alters the inhibitory mechanism of plasminogen activator inhibitor-1. *Biochemistry* **42,** 12260–12272
20. Deutsch, D. G., and Mertz, E. T. (1970) Plasminogen. Purification from human plasma by affinity chromatography. *Science* **170,** 1095–1096
21. Futamura, A., and Gettins, P. G. (2000) Serine 380 (P14) → glutamate mutation activates antithrombin as an inhibitor of factor Xa. *J. Biol. Chem.* **275,** 4092–4098
22. Driever, W., and Rangini, Z. (1993) Characterization of a cell line derived from zebrafish (*Brachydanio rerio*) embryos. *In Vitro Cell. Dev. Biol. Anim.* **29,** 749–754
23. Culp, P. A. (1994) Random DNA integrations as an approach to insertional mutagenesis in the zebrafish (*Brachydanio rerio*). Ph.D. thesis, Massachusetts Institute of Technology
24. Braun-Nesje, R., Bertheussen, K., Kaplan, G., and Seljelid, R. (1981) Salmonid macrophages. Separation, *in vitro* culture, and characterization. *J. Fish Dis.* **4,** 141–151
25. Pettersen, E. F., Bjerknes, R., and Wergeland, H. I. (2000) Studies of Atlantic salmon (*Salmo salar* L.) blood, spleen, and head kidney leucocytes using specific monoclonal antibodies, immunohistochemistry and flow cytometry. *Fish Shellfish Immunol.* **10,** 695–710
26. Arnold, K., Bordoli, L., Kopp, J., and Schwede, T. (2006) The SWISS-MODEL workspace. A web-based environment for protein structure homology modeling. *Bioinformatics* **22,** 195–201
27. UniProt, C. (2011) Ongoing and future developments at the Universal Protein Resource. *Nucleic Acids Res.* **39,** D214–219
28. Pruitt, K. D., Tatusova, T., and Maglott, D. R. (2005) NCBI reference sequence (RefSeq). A curated nonredundant sequence database of genomes, transcripts, and proteins. *Nucleic Acids Res.* **33,** D501–504
29. Dsouza, M., Larsen, N., and Overbeek, R. (1997) Searching for patterns in genomic data. *Trends Genet.* **13,** 497–498
30. Petersen, L. C., Lund, L. R., Nielsen, L. S., Danø, K., and Skriver, L. (1988) One-chain urokinase-type plasminogen activator from human sarcoma cells is a proenzyme with little or no intrinsic activity. *J. Biol. Chem.* **263,** 11189–11195
31. Andreasen, P. A., Petersen, L. C., and Danø, K. (1991) Diversity in catalytic properties of single chain and two chain tissue-type plasminogen activator. *Fibrinolysis* **5,** 207–215
32. Vassalli, J. D., and Belin, D. (1987) Amiloride selectively inhibits the urokinase-type plasminogen activator. *FEBS Lett.* **214,** 187–191
33. Ploug, M., Ostergaard, S., Hansen, L. B., Holm, A., and Danø, K. (1998) Photoaffinity labeling of the human receptor for urokinase-type plasminogen activator using a decapeptide antagonist. Evidence for a composite ligand-binding site and a short interdomain separation. *Biochemistry* **37,** 3612–3622
34. Lin, Z., Jiang, L., Yuan, C., Jensen, J. K., Zhang, X., Luo, Z., Furie, B. C., Furie, B., Andreasen, P. A., and Huang, M. (2011) Structural basis for recognition of urokinase-type plasminogen activator by plasminogen activator inhibitor-1. *J. Biol. Chem.* **286,** 7027–7032
35. Appella, E., Robinson, E. A., Ullrich, S. J., Stoppelli, M. P., Corti, A., Cassani, G., and Blasi, F. (1987) The receptor-binding sequence of urokinase. A biological function for the growth factor module of proteases. *J. Biol. Chem.* **262,** 4437–4440
36. Huai, Q., Mazar, A. P., Kuo, A., Parry, G. C., Shaw, D. E., Callahan, J., Li, Y., Yuan, C., Bian, C., Chen, L., Furie, B., Furie, B. C., Cines, D. B., and Huang, M. (2006) Structure of human urokinase plasminogen activator in complex with its receptor. *Science* **311,** 656–659
37. Lin, L., Gårdsvoll, H., Huai, Q., Huang, M., and Ploug, M. (2010) Structure-based engineering of species selectivity in the interaction between urokinase and its receptor. Implication for preclinical cancer therapy. *J. Biol. Chem.* **285,** 10982–10992
38. Barinka, C., Parry, G., Callahan, J., Shaw, D. E., Kuo, A., Bdeir, K., Cines,

D. B., Mazar, A., and Lubkowski, J. (2006) Structural basis of interaction between urokinase-type plasminogen activator and its receptor. *J. Mol. Biol.* **363,** 482–495

39. Barnham, K. J., Torres, A. M., Alewood, D., Alewood, P. F., Domagala, T., Nice, E. C., and Norton, R. S. (1998) Role of the 6–20 disulfide bridge in the structure and activity of epidermal growth factor. *Protein Sci.* **7,** 1738–1749
40. Behrendt, N., Ronne, E., and Dano, K. (1996) Domain interplay in the urokinase receptor. Requirement for the third domain in high affinity ligand binding and demonstration of ligand contact sites in distinct receptor domains. *J. Biol. Chem.* **271,** 22885–22894
41. Pébusque, M. J., Coulier, F., Birnbaum, D., and Pontarotti, P. (1998) Ancient large-scale genome duplications. Phylogenetic and linkage analyses shed light on chordate genome evolution. *Mol. Biol. Evol.* **15,** 1145–1159
42. Putnam, N. H., Butts, T., Ferrier, D.E., Furlong, R. F., Hellsten, U., Kawashima, T., Robinson-Rechavi, M., Shoguchi, E., Terry, A., Yu, J. K., Benito-Gutiérrez, E. L., Dubchak, I., Garcia-Fernàndez, J., Gibson-Brown, J. J., Grigoriev, I. V., Horton, A. C., de Jong, P. J., Jurka, J., Kapitonov, V. V., Kohara, Y., Kuroki, Y., Lindquist, E., Lucas, S., Osoegawa, K., Pennacchio, L. A., Salamov, A. A., Satou, Y., Sauka-Spengler, T., Schmutz, J., Shin-I, T., Toyoda, A., Bronner-Fraser, M., Fujiyama, A., Holland, L. Z., Holland, P. W., Satoh, N., and Rokhsar, D. S. (2008) The amphioxus genome and the evolution of the chordate karyotype. *Nature* **453,** 1064–1071
43. Wouters, M. A., Rigoutsos, I., Chu, C. K., Feng, L. L., Sparrow, D. B., and Dunwoodie, S. L. (2005) Evolution of distinct EGF domains with specific functions. *Protein Sci.* **14,** 1091–1103
44. Jaillon, O., Aury, J. M., Brunet, F., Petit, J. L., Stange-Thomann, N., Mauceli, E., Bouneau, L., Fischer, C., Ozouf-Costaz, C., Bernot, A., Nicaud, S., Jaffe, D., Fisher, S., Lutfalla, G., Dossat, C., Segurens, B., Dasilva, C., Salanoubat, M., Levy, M., Boudet, N., Castellano, S., Anthouard, V., Jubin, C., Castelli, V., Katinka, M., Vacherie, B., Biémont, C., Skalli, Z., Cattolico, L., Poulain, J., De Berardinis, V., Cruaud, C., Duprat, S., Brottier, P., Coutanceau, J. P., Gouzy, J., Parra, G., Lardier, G., Chapple, C., McKernan, K. J., McEwan, P., Bosak, S., Kellis, M., Volff, J. N., Guigó, R., Zody, M. C., Mesirov, J., Lindblad-Toh, K., Birren, B., Nusbaum, C., Kahn, D., Robinson-Rechavi, M., Laudet, V., Schachter, V., Quetier, F., Saurin, W., Scarpelli, C., Wincker, P., Lander, E. S., Weissenbach, J., and Roest Crollius, H. (2004) Genome duplication in the teleost fish *Tetraodon nigroviridis* reveals the early vertebrate proto-karyotype. *Nature* **431,** 946–957
45. Carmeliet, P., Moons, L., Dewerchin, M., Rosenberg, S., Herbert, J. M., Lupu, F., and Collen, D. (1998) Receptor-independent role of urokinase-type plasminogen activator in pericellular plasmin and matrix metalloproteinase proteolysis during vascular wound healing in mice. *J. Cell Biol.* **140,** 233–245
46. Stempien-Otero, A., Plawman, A., Meznarich, J., Dyamenahalli, T., Otsuka, G., and Dichek, D. A. (2006) Mechanisms of cardiac fibrosis induced by urokinase plasminogen activator. *J. Biol. Chem.* **281,** 15345–15351
47. Wei, C., Möller, C. C., Altintas, M. M., Li, J., Schwarz, K., Zacchigna, S., Xie, L., Henger, A., Schmid, H., Rastaldi, M. P., Cowan, P., Kretzler, M., Parrilla, R., Bendayan, M., Gupta, V., Nikolic, B., Kalluri, R., Carmeliet, P., Mundel, P., and Reiser, J. (2008) Modification of kidney barrier function by the urokinase receptor. *Nat. Med.* **14,** 55–63
48. Rivière, S., Challet, L., Fluegge, D., Spehr, M., and Rodriguez, I. (2009) Formyl peptide receptor-like proteins are a novel family of vomeronasal chemosensors. *Nature* **459,** 574–577
49. Bøtkjaer, K. A., Byszuk, A. A., Andersen, L. M., Christensen, A., Andreasen, P.A., and Blouse, G. E. (2009) Nonproteolytic induction of catalytic activity into the single-chain form of urokinase-type plasminogen activator by dipeptides. *Biochemistry* **48,** 9606–9617